# Dynamics of Fullerene–Mediated Heat–Driven Release of Drug Molecules from Carbon Nanotubes

**ARTICLE** *in* JOURNAL OF PHYSICAL CHEMISTRY LETTERS · NOVEMBER 2013

Impact Factor: 7.46 · DOI: 10.1021/jz402231p

THE JOURNAL OF PHYSICAL CHEMISTRY Letters

Letter

pubs.acs.org/JPCL

# Dynamics of Fullerene-Mediated Heat-Driven Release of Drug Molecules from Carbon Nanotubes

Nabanita Saikia,[†] Anupam Nath Jha,[‡] and Ramesh Ch. Deka*[,†]

[†]Department of Chemical Sciences and [‡]Department of Molecular Biology and Biotechnology, Tezpur University, Napaam, Tezpur, Assam 784 028, India

Supporting Information

**ABSTRACT:** We have performed molecular dynamics (MD) simulations as a function of temperature to investigate the controlled release of multiple pyrazinamide (PZA) drug molecules encapsulated within single-wall carbon nanotube (SWCNT) mediated by fullerene ($C_{60}$) fillers. The displacement of PZA by $C_{60}$ can be accounted to the comparatively higher $\pi-\pi$ stacking between $C_{60}$–SWCNT and PZA–SWCNT. The root-mean-square deviation (RMSD) provides definitive insight into drug release and simultaneous $C_{60}$ entrapment within the nanotube. The diffusion coefficient, variation of center of mass (COM), and energetic profiles at different temperatures suggest that the rate of diffusion of PZA increases with temperature. These results can be quite instrumental in providing details about the role of temperature on drug release from confined SWCNTs and aims at achieving the drug delivery regime.

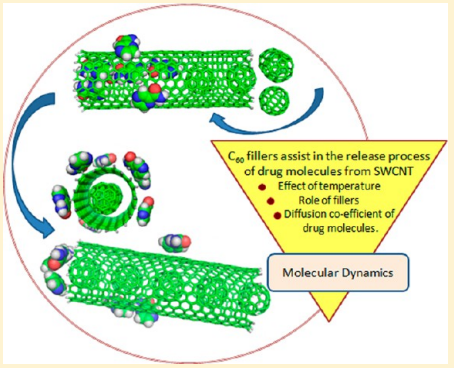


**SECTION:** Physical Processes in Nanomaterials and Nanostructures

One-dimensional nanomaterials like single-wall carbon nanotubes (SWCNTs) draw considerable research interest accounted mainly from their unique structure as well as the electronic properties. Unlike the other class of graphene-based nanomaterials, SWCNTs facilitate the interaction of various molecules both along the sidewall and within the hollow cylindrical cavity (endohedral), leading to the formation of quasi-1D arrays.[1] Compared to sidewall functionalization, which makes the organic and biologically active molecules prone (vulnerable) to the biological environment, encapsulation provides a sought after alternative toward restoring the activity of the molecules and preventing any undesirable degradation of its properties. The noteworthy prospects of using SWCNTs as carrier payloads for systematic loading and delivery of therapeutic agents at the target site of action can be accounted to its cylindrical needle-like structure that can simply penetrate the cell membrane (nano inject) and transfer the cellular components with reduced side effects.[2−4] A CNT with its intrinsic structural properties in addition to its ability to absorb near-infrared (NIR) radiation (800−1100 nm)[5] along with Raman and photoluminescence properties exhibits additional advantages such as the real time monitoring of in vivo drug trafficking.[6] The NIR laser irradiation can heat up and destroy malignant tumor cells preconjugated with SWCNTs as most living organisms are transparent to NIR irradiation.[7] With the implementation of advanced nanotechnology to nanomedicine, the targeted delivery of pharmaceutical compounds to specific cellular and intracellular sites within the human body has become possible.[8]

The formation of fullerene arrays within the hollow cavity of a SWCNT was first observed by Smith et al. in 1998 using high-resolution transmission electron microscopy (HRTEM).[9] Buckminster fullerenes or buckyballs ($C_{60}$) were the first studied molecules for encapsulation within SWCNTs. Because of the similarity in structural motif and uniform center-to-center distances, the fullerene molecules encapsulated within the nanotubes are popularly known as "peapods".[10] The encapsulation of fullerene inside of CNTs is quite spontaneous, irreversible, dependent on nanotube diameter, and exothermic, such that the resultant $\pi-\pi$ interaction stabilizes the host–guest structure.[11] Xue et al. investigated the release of encapsulated molecules within CNTs by $C_{60}$ fillers through a displacement process that is attributed to the vdW interaction between the nanotube and filler molecules rather than the nanotube and encapsulated molecules.[12] Similarly, Gao et al.[13] analyzed the spontaneous encapsulation of DNA oligonucleotides within SWCNTs and showed that the vdW forces play a major dominant role. In nanofluidic device applications,[14,15] nanoporous materials like CNTs make possible the confinement of gaseous molecules within the hollow cavity.[16,17] Prezdo and co-workers in a very comprehensive way investigated the effects of spatial confinement on the evaporation and vapor pressure of encapsulated water droplets inside of a CNT.[18,19] Panczyk et al.[20] exploited a completely new approach toward the dynamics of release of cisplatin anticancer drugs confined within a SWCNT precapped with magnetic nanoparticles. The time scale for drug release depends on the length of the

**Received:** October 16, 2013
**Accepted:** November 19, 2013
**Published:** November 19, 2013

   dx.doi.org/10.1021/jz402231p | J. Phys. Chem. Lett. 2013, 4, 4126−4132

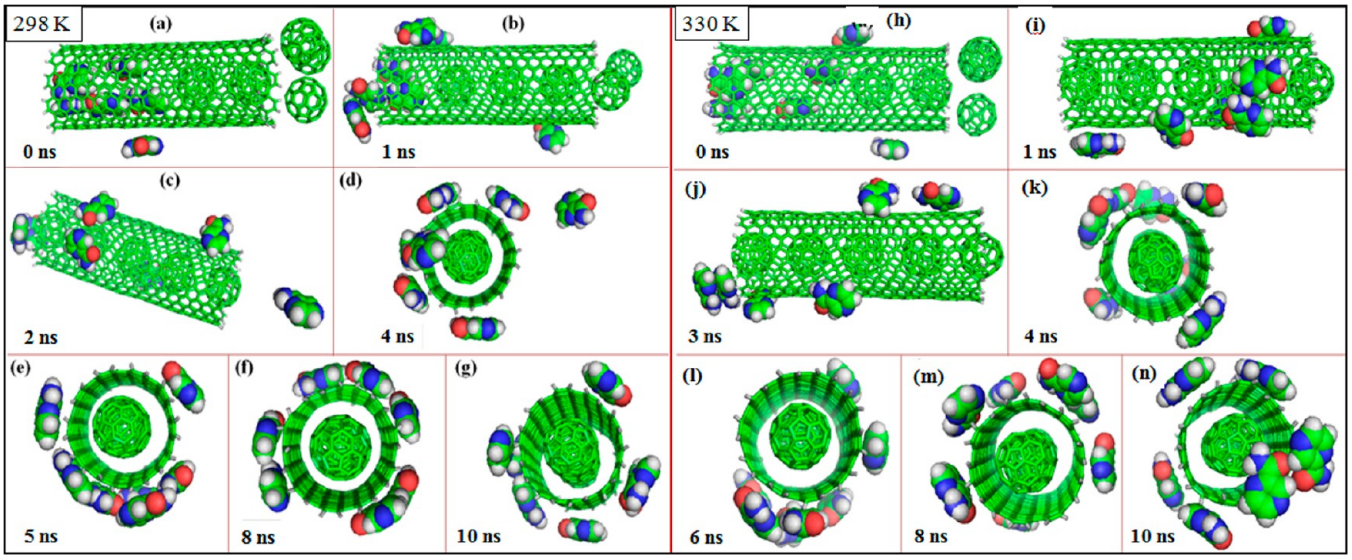


**Figure 1.** Simulation snapshots corresponding to the release of PZA molecules encapsulated within the (10,10) SWCNT at 298 K for (a) 0, (b) 1, (c) 2, (d) 4, (e) 5, (f) 8, and (g) 10 ns; simulation snapshots corresponding to the release of PZA molecules from the (10,10) SWCNT at 330 K temperature for (h) 0, (i) 1, (j) 3, (k) 4, (l) 6, (m) 8, and (n) 10 ns.

nanotube, the amount of encapsulated molecules, and the rate of diffusivity of cisplatin inside of the CNT.

Contemplating the vast potential that the subject area has to offer, with opening up new challenging avenues in the field of biomedical research, we attempt to incorporate the properties of a fullerene−SWCNT conjugated system to investigate the controlled heat-driven release of multiple pyrazinamide (PZA) antitubercular drug molecules encapsulated within a SWCNT by fullerene $C_{60}$ fillers using a mutual displacement mechanism. The drug release process has been investigated at higher temperatures to mimic the physiological scenario of heating a SWCNT precapsulated with biomolecules using NIR radiation. The observed parameters at different temperatures, namely, the root-mean-square deviation (RMSD), variation in center of mass (COM), the diffusion coefficient of PZA from a SWCNT, along with the energetics profile can help in comprehending the temperature effect in the drug release process. The choice for $C_{60}$ as the fillers for replacing PZA molecules entrapped within a SWCNT is multifold; first, due to the small diameter (∼6.978 Å) and confined $\pi$-electron framework, the encapsulation is quite flexible, and second, $C_{60}$ holds foremost biological importance.[21−23] Multiple loading and subsequent delivery of chemotherapeutics from SWCNTs can help enhance the therapeutic efficacy along with sustained drug retention time within the nanotube, and temperature forms the driving parameter that controls the rate of drug release, which we highlight in our study. High temperature mimics the scenario of irradiating nanotubes for active drug release at the target site in the body. All of the calculations are performed using the GROMACS 4.5.0 program with the OPLS−AA force field[24] for the system comprised of SWCNTs, PZA, and $C_{60}$ filler molecules at five different temperatures (298, 300, 310, 330, and 337 K). A SWCNT of chirality (10,10) having a diameter of 14.652 Å and length of 45.812 Å was chosen for the study. The force field parameters for the carbon and hydrogen atoms in a SWCNT and $C_{60}$ are provided in Table S1 of the Supporting Information. The simulation system consists of a (10,10) SWCNT with seven encapsulated PZA molecules forming a cluster along the central region of the nanotube, depicting a scenario wherein the nanotube filled with drug molecules has been delivered to the target cells but not unloaded. At the initial configuration, five filler molecules were placed close to the entering path along one of the nanotube open axes with the entrapped PZA molecules intact. The choice for the five $C_{60}$ fillers is based on the optimum number of fillers required to completely encapsulate inside of the nanotube of the optimum length considered in the study. The complete details of the computational method are provided in the Supporting Information.

The optimized geometries of the PZA drug, $C_{60}$ filler, (10,10) SWCNT, and (14,14) SWCNT are represented in the Supporting Information, Figure S1. PZA is a planar molecule (Figure S1a) with the $-CONH_2$ lying in the molecular plane of the pyrazine ring. The optimum lengths and diameters of the (10,10) and (14,14) SWCNTs are described in Figure S1b and c (Supporting Information). Figure 1 depicts the stepwise process of gradual release of PZA molecules encapsulated within the (10,10) SWCNT at 298 K (corresponding to room temperature of 25 °C).

Within the time frame of 1−2 ns, complete encapsulation of all five $C_{60}$ fillers is accompanied by release of the PZA molecules from the nanotube cavity (Figure 1c). The diameter of the (10,10) SWCNT considered for the study is thus optimum enough to hold the $C_{60}$ molecules, but space restriction hinders the encapsulation of PZA or water molecules simultaneously along with $C_{60}$. The release of PZA with concurrent encapsulation of $C_{60}$ is quite prompt at 298 K, taking place at around 1−2 and 2−10 ns of simulation (Figure 1d−g); the fillers prefer to remain within the nanotube cavity accounted mainly to the strong $\pi\cdots\pi$ and $CH\cdots\pi$ interactions with the nanotube sidewall. Interestingly, PZA molecules form a uniform array along the tube sidewall, as observed from the snapshots, mediated by the strong $\pi-\pi$ stacking interaction of the pyrazine ring of PZA with the nanotube.

A similar trend was observed at 300 and 310 K, (Supporting Information, Figures S2 and S3), and filling of $C_{60}$ inside of the SWCNT bears a parametric dependence on temperature. The rate of encapsulation of the fullerene gets enhanced at higher


dx.doi.org/10.1021/jz402231p | J. Phys. Chem. Lett. 2013, 4, 4126−4132

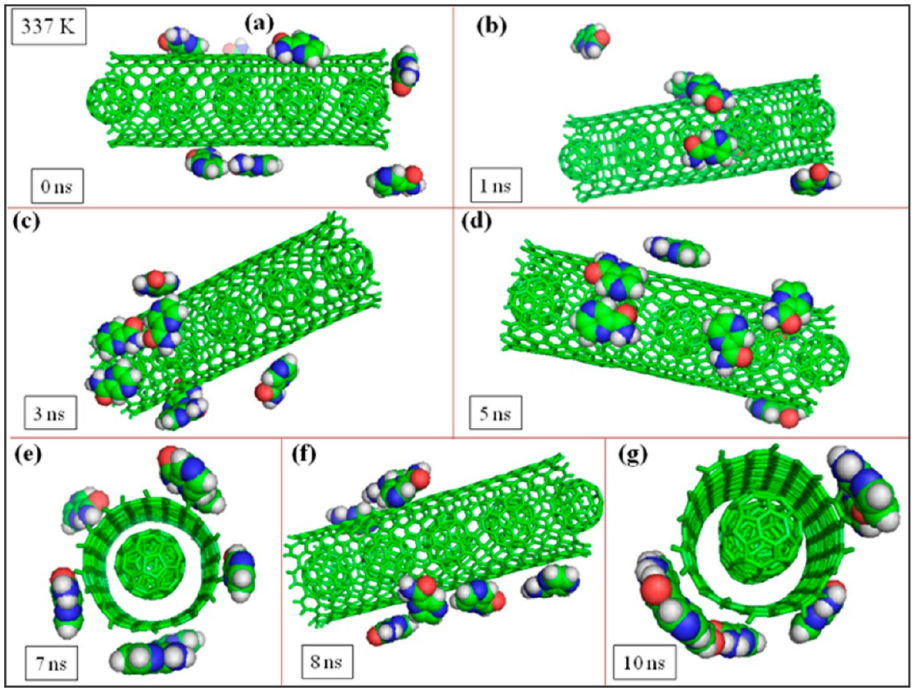


**Figure 2.** Simulation snapshots corresponding to the release of PZA molecules encapsulated within the (10,10) SWCNT at (a) 0, (b) 1, (c) 3, (d) 5, (e) 7, (f) 8, and (g) 10 ns, corresponding to 337 K.

temperatures (330 and 337 K) wherein all of the filler molecules pack inside of the SWCNT within the first 1 ns at 330 K (57 °C) (Figure 1h and i). A further 7° rise in temperature to 337 K (corresponding to 64 °C) (Figure 2) demonstrates quite an interesting trend with the complete encapsulation of all five $C_{60}$ fillers taking place at the start of the simulation, and the PZA molecules prefer to remain stacked along the tube sidewall (Figure 2b–g) mediated by the noncovalent $\pi$-stacking interaction with fewer fluctuations.

At room temperature (298 K) and normal body temperature (310 K), although fullerene is capable of expelling PZA from the SWCNT, overcoming the potential energy barrier imposed by PZA molecules, there is a time lag associated with the drug release process. The temperature factor bears a monotonic relation with the PZA diffusion rate, which can be explained from the kinetic theory of gases. An increase in temperature elevates the available degrees of freedom of the less bulky PZA molecules compared to the robust $C_{60}$ or SWCNT, thereby promoting the fillers to overcome the energy barrier and fill the nanotube.

For a quantitative understanding of the dynamics of PZA release, we compared the RMSD for three components of the system, $C_{60}$, PZA, and SWCNT−$C_{60}$−PZA combined. At 298 K (Figure 3a) between 0 and 1.2 ns, the RMSD gradually increases, accompanied with more fluctuations in the RMSD for PZA compared to that of the bulky $C_{60}$ and SWCNT.

The steady increase in the RMSD between 0 and 1.3 ns is due to rapid shuffling of PZA inside of a SWCNT, and the sudden jump in the RMSD (maximum value of around 3.0 nm) between 1.5 and 3.1 ns is accounted to the complete release of the PZA molecules by $C_{60}$ fillers. The patterns of the RMSD observed at 300 (Supporting Information, Figure S4) and 310 K (Figure 3b) are quite similar in nature. The sudden steep increase in the RMSD around 4.3 ns for 300 K and 2.5 ns for 310 K corresponds to the point of complete encapsulation of the fillers and expulsion of all seven PZA molecules from the nanotube. The RMSD at 330 K (Figure 3c) demonstrates rapid encapsulation of $C_{60}$ fillers within the first 500 ps (0.5 ns), suggesting that temperature pops up the course of drug release and instantaneous fullerene mediation. The RMSD of the combined system and $C_{60}$ fillers increases and then remains uniform at average values of 1.25 and 1.13 nm, respectively. The RMSD for PZA initially increases and obtains an average value of 1.5 nm until 6.5 ns, and a sudden sharp peak in the RMSD (~3.75 nm) is observed at around 7.5 ns, which normalizes up to the completion of simulation. The RMSD of $C_{60}$ fillers at 337 K (Figure 3d) maintains an average value of 0.30 nm because the fillers are already encapsulated at the start of the simulation itself, whereas for PZA, it demonstrates significant fluctuations, initially increasing from 0 to 1.0 ns and then more or less saturating at around 2.35 nm. The RMSD of the combined system follows a similar trend as that of PZA and lies between the values of PZA molecules and $C_{60}$ at around 0.85 nm. It is quite interesting to point out that the RMSD for $C_{60}$ at 337 K is lower in value compared to those at the other studied temperatures, and the probable reason may be that at 337 K, the fillers are already encapsulated and hence in absence of any energy barrier imposed by the presence of PZA molecules; the perturbations are lower, hence, the observed low value in the RMSD.

In addition, we computed the disparity in the COM distances between $C_{60}$−SWCNT and PZA−SWCNT to comprehend the distance variation between the interacting groups during the course of simulation, as depicted in Figure 4.

At 298 K (Figure 4a), the COM distance of PZA−(10,10) SWCNT for the first 0.6 ns remains slightly below 1.25 nm, and between 0.65 and 1.0 ns, the COM distance suddenly drops to 0.18 nm, followed by the sharp increase in distance to 1.75 nm beyond 1.35 ns. The trends in variation in the COM distance at 300 (Figure 4b) and 310 K (Supporting Information, Figure S5a) are comparable to those at 298 K, with the fluctuation taking place at around 4.0 ns for 300 K and 2.35 ns at 310 K,


dx.doi.org/10.1021/jz402231p | J. Phys. Chem. Lett. 2013, 4, 4126−4132

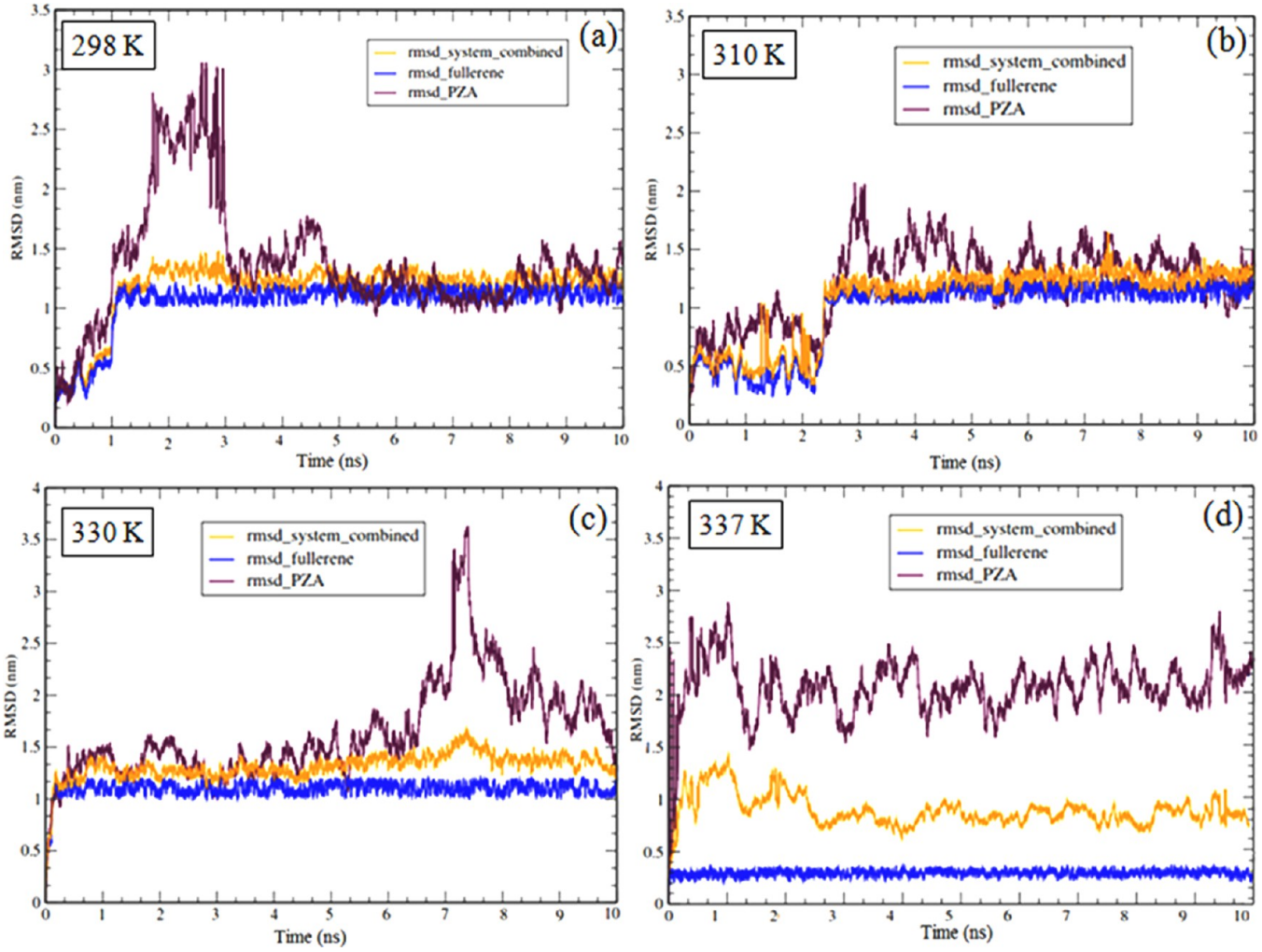


**Figure 3.** The RMSD plots of PZA, $C_{60}$ fillers, and PZA−$C_{60}$−SWCNT combined at (a) 298, (b) 310, (c) 330, and (d) 337 K.

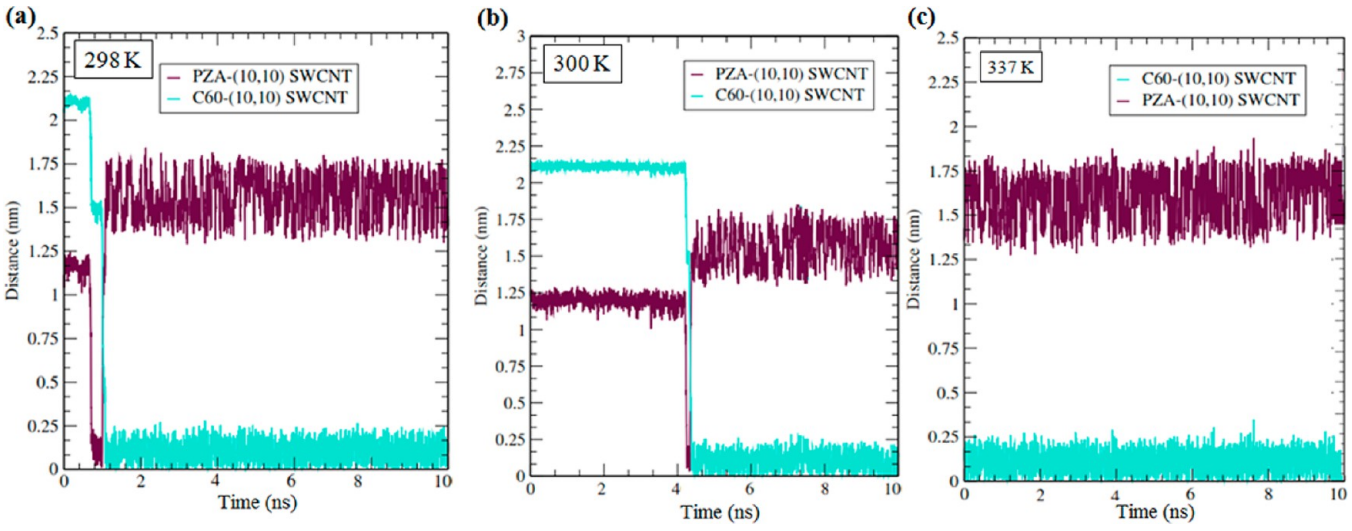


**Figure 4.** The variation of the COM between PZA−(10,10) SWCNT and $C_{60}$−SWCNT at (a) 298, (b) 300, and (c) 337 K.

corresponding to complete filling of $C_{60}$ arrays within the SWCNT. At 330 (Supporting Information, Figures S5b) and 337 K (Figure 4c), the COM distances do not show any major fluctuations in values, and the average COM distances between $C_{60}$−SWCNT and PZA−SWCNT are observed at around 0.23 and 1.75 nm, respectively. The trends in the COM variation at 330 and 337 K illustrate that at elevated temperatures, the $C_{60}$ fillers obtain the energetically favorable state within the nanotube at the start of the simulation itself, and removal of all PZA molecules results in no predominant variation in


dx.doi.org/10.1021/jz402231p | J. Phys. Chem. Lett. 2013, 4, 4126−4132

distance. The average COM distance is almost similar in value at the five studied temperatures once complete encapsulation of fullerene occurs, and the extended delocalized framework of the SWCNT holds the fillers as well as the PZA molecules along the nanotube sidewall.

To assess the feasibility of self-diffusion of PZA molecules from SWCNTs in the absence of fillers, Figure S6 (Supporting Information) depicts the simulation snapshots of the PZA−SWCNT system at 298 K. In the absence of any external driving agent, PZA molecules assume a thermodynamically (energetically) favorable situation by preferring to remain stacked onto the tube sidewall mediated by the noncovalent vdW interactions. The RMSD of the (10,10) SWCNT does not exhibit any perturbation at an average value of 0.05 nm (Supporting Information, Figure S7a). The RMSD of PZA molecules however contributes to the major fluctuations, increasing initially for the first 500 ps and then reaching a plateau at around 0.56 nm. The RMSD for the combined system lies between the values of PZA and the (10,10) SWCNT at around 0.2 nm. The COM distance between PZA and SWCNT (Figure S7b, Supporting Information) also shows significant oscillations at distances between 0.05 and ∼0.8 nm, and the average interacting distance is calculated at around 0.52 nm.

MD simulation of $C_{60}$−SWCNT without PZA molecules (Figure S8a−f, Supporting Information) depicts instantaneous irreversible encapsulation of $C_{60}$ fillers within the SWCNT at the start of the simulation. The strong $\pi-\pi$ interaction between $C_{60}$ and SWCNT leads to rapid trafficking of the fillers inside of the nanotube, and because there is no posed hindrance, the encapsulation is quite instantaneous (occurring at 0 ns itself). The average COM distance of $C_{60}$ and SWCNT obtained at around 0.40 nm (Supporting Information, Figure S8g) is slightly higher than the COM distance calculated in the presence of PZA molecules (e.g., Figure 4). The probable justification toward the trend may be that in the presence of PZA molecules, the interaction is via a mutual cooperative (competitive) effect due to which the COM distance is somewhat lower than the values obtained for the former. Overall, the individual simulations of PZA−SWCNT and $C_{60}$−SWCNT systems at 298 K demonstrate the strong dependence of fillers in the release process of PZA, and in the absence of any external drive, PZA molecules favor to remain in the energetically favorable encapsulated state.

To get a physical sense of PZA liberation from the SWCNT, we compared the diffusion coefficient of PZA molecules as a function of temperature, as illustrated in Figure 5. For a 2 K increment in temperature from 298 to 300 K, the diffusion coefficient of PZA at 298 K is higher than that at 300 K, and this deflection in trend can be correlated from RMSD plots that show that at 298 K, diffusion of all of the PZA molecules from the SWCNT occurs at around 1.1 ns whereas at 300 K, it takes place at ∼4.1 ns, suggesting that complete removal of PZA molecules at 300 K is somewhat lower than that at 298 K, and above 300 K, the diffusion coefficient value increases steadily.

To present a better correlation for the deflection in diffusion coefficient values between 298 and 300 K, we calculated the diffusion coefficient for the same studied system at 290 K and observed that PZA diffusion from the SWCNT is comparatively slower below room temperature as opposed to that at the higher temperatures. Overall, temperature elevation facilitates the spontaneous insertion of $C_{60}$ fillers, and irradiation of the SWCNT assists in better drug discharge from the SWCNT.

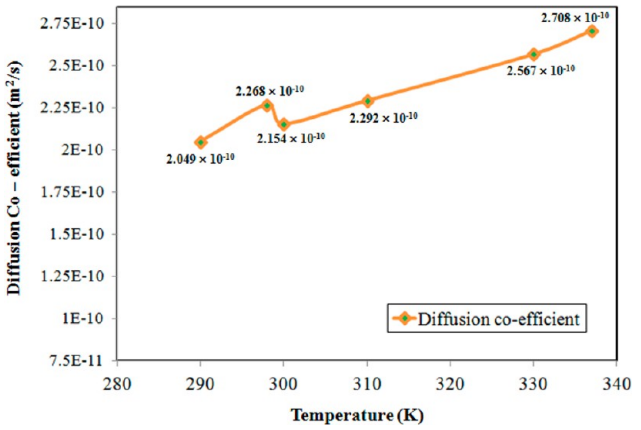


**Figure 5.** The diffusion coefficient of PZA molecules from the SWCNT at 290, 298, 300, 310, 330, and 337 K.

The small deflection from the exponential behavior for the temperature range of 290−300 K can be attributed to the thermal fluctuations in the system with temperature in addition to the general uncertainties in the diffusion constant.[25]

From energetics perspective, the total energy of the system increases with an increase in temperature (Table S2 and Figure S9, Supporting Information), and the calculated energy values are quite high due to the large number of atoms in the system (1118 atoms excluding the 75513 atoms of water molecules). The nonbonded vdW term basically contributes toward the energetics, and the interaction energy increases with an increase in temperature, which can be correlated with the temperature effect on rapid encapsulation. The potential energy however decreases with an increase in temperature, which is associated with the increase in contact area between $C_{60}$ fillers and the SWCNT and suggests that the release of PZA molecules is a process of energy minimization, which is in accordance with the lowest energy theory.[26] Overall, the negative energy values highlight the thermodynamic favorability toward the encapsulation and the process of drug release. The energy profiles corresponding to the total and potential energy values at the five temperatures are provided in the Supporting Information, Figures S10−S14.

The heat-driven release process of PZA molecules was further extended to a larger-diameter (14,14) SWCNT at 298 and 330 K, the simulation snapshots of which are provided in Figure 6. At the two investigated temperatures, we observe quite an interesting phenomenon where the filler molecules forcibly encapsulate within the nanotube, which leads to the buckling or deformation in the nanotube structural framework, and the perfect cylindrical structure is lost. The temperature effect is of less predominance here because at the start of the simulation itself (0 ns) (Figure 6a and f), all of the fillers fill the nanotube cavity, forming a double array irrespective of temperature, and from there on until the completion of the simulation, the major fluctuations observed are in the position of PZA molecules around the (14,14) SWCNT.

For nanotubes with a larger diameter, the force constraint for fullerene encapsulation is less hindered, which eases the trafficking of the fillers inside of the nanotube, whereas for the (10,10) SWCNT, the diameter is optimum to hold a uniform single array, which also adds to the lesser deformation in narrow diameter nanotubes. Thus, for nanotubes with a much larger diameter, the role of temperature is of less predominance, and the drug release is quite spontaneous


dx.doi.org/10.1021/jz402231p | J. Phys. Chem. Lett. 2013, 4, 4126−4132

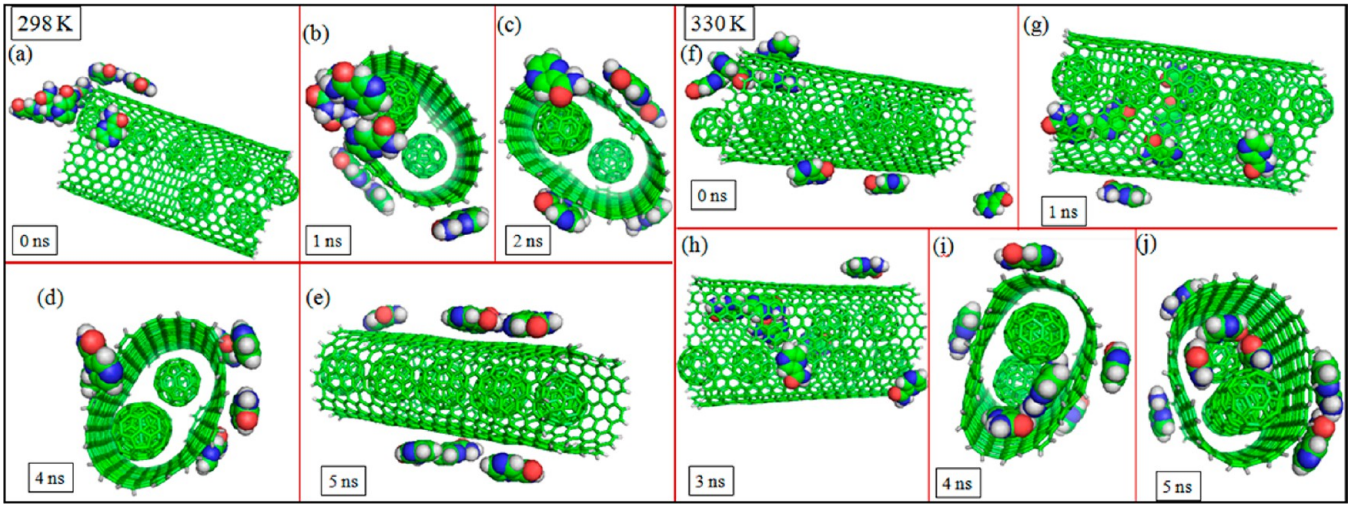


**Figure 6.** Simulation snapshots of release of PZA molecules encapsulated within the (14,14) SWCNT mediated by $C_{60}$ fillers at (a) 0, (b) 1, (c) 2, (d) 4, and (e) 5 ns, corresponding to 298 K. Simulation snapshots of release of PZA molecules encapsulated within the (14,14) SWCNT at (f) 0, (g) 1, (h) 3, (i) 4, and (j) 5 ns, corresponding to 330 K.

irrespective of the system temperature. Our choice for considering the (10,10) SWCNT is supported in an earlier reported study by Coluci and co-workers,[27] wherein they investigated the formation of ordered fullerene arrays inside of a SWCNT as a function of nanotube diameter. Their study clearly highlighted the point that the smallest tube where $C_{60}$ molecules can be encapsulated to form linear chains without deformation is the (10,10) SWCNT, which is also in good agreement with previous experimental[9,26] and theoretical[11,28] studies, and the process of encapsulation is exothermic for the (10,10) SWCNT. For nanotubes having a larger diameter, fullerene molecules can form a number of different arrays depending on the nature of packing, namely, zigzag, double and triple helices, double helix, and so on. The only difference with their study was that in all of the simulations, the SWCNT did not undergo any structural deformations, and in the (14,14) SWCNT, $C_{60}$ molecules form a zigzag pattern, but in our study, we clearly observe that in the (14,14) SWCNT, fullerene molecules compulsively form a double array, leading to deformation of the tube structure, suggesting the flexibility of the SWCNT toward the encapsulation of $C_{60}$.

In conclusion, we have designed SWCNTs as carrier depots for PZA chemotherapeutics and investigated the role of external fillers in the drug release process. Temperature bears a strong correlation with PZA delivery for nanotubes with a narrow diameter like in the (10,10) SWCNT; an increase in temperature leads to rapid drug diffusion from the nanotube and spontaneous encapsulation of $C_{60}$ molecules. The major fluctuation in the RMSD is contributed to the less bulky PZA compared to $C_{60}$ or the SWCNT. The COM distance increases for PZA−SWCNT and decreases for $C_{60}$−SWCNT as the simulation proceeds. The diffusion of PZA molecules increases with temperature, suggesting the strong dependence of temperature in the pace of PZA release and from the energetics viewpoint; the nonbonded vdW interactions play the determining role. For nanotubes with a larger diameter, the temperature effect is of less predominance, and fullerene encapsulation results in the deformation of nanotubes in order to accommodate the fillers, and the drug release is spontaneous irrespective of the applied temperature. However, it is noteworthy to point out here that the major concerns raised about nanotube cytotoxicity primarily apply to longer nanotubes with larger diameters; therefore, for effectual drug delivery pursuits, the choice of an optimum length and diameter of the SWCNT is the most crucial part from the drug delivery perspective.

## ■ ASSOCIATED CONTENT

### Supporting Information

Computational details, force field parameters for carbon atoms in the SWCNT, energy parameters for the studied systems, optimized geometries of PZA, SWCNTs, and the $C_{60}$ filler molecule, simulation snapshots at 300 and 310 K, the RMSD plot at 300 K, variation of center of mass distances at 310−330 K, simulation snapshots, RMSD and variation in the COM distance for PZA−SWCNT at 298 K, simulation snapshots and variation in the COM distance for $C_{60}$−SWCNT at 298 K, energy profiles for the total and potential energy values at the five studied temperatures. This material is available free of charge via the Internet at http://pubs.acs.org.

## ■ AUTHOR INFORMATION

### Corresponding Author

*E-mail: ramesh@tezu.ernet.in. Fax: 913712267005. Tel: 913712267008.

### Notes

The authors declare no competing financial interest.

## ■ ACKNOWLEDGMENTS

The project is funded from the Department of Science and Technology (DST), India, and N.S. acknowledges The Council of Scientific and Industrial Research (CSIR) for the Senior Research Fellowship (SRF).

## ■ REFERENCES

(1) Khlobystov, A. N.; Britz, D. A.; Briggs, G. A. D. Molecules in Carbon Nanotubes. *Acc. Chem. Res.* **2005**, *38*, 901−909.

(2) Pantarotto, D.; Briand, J. P.; Prato, M.; Bianco, A. Translocation of Bioactive Peptides Across Cell Membranes by Carbon Nanotubes. *Chem. Commun.* **2004**, *10*, 16−17.

(3) Kam, N. W. S.; Liu, Z.; Dai, H. Carbon Nanotubes As Intracellular Transporters for Proteins and DNA: An Investigation of the Uptake Mechanism and Pathway. *Angew. Chem.* **2005**, *44*, 1−6.
(4) Cai, D.; Mataraza, J. M.; Qin, Z. H. Highly Efficient Molecular Delivery into Mammalian Cells Using Carbon Nanotube Spearing. *Nat. Methods* **2005**, *2*, 449−454.
(5) Carlson, L. J.; Krauss, T. D. Photophysics of Individual Single-Walled Carbon Nanotubes. *Acc. Chem. Res.* **2008**, *41*, 235−243.
(6) Liu, Z.; Robinson, J. T.; Tabakman, S. M.; Yang, K.; Dai, H. Carbon Materials for Drug Delivery & Cancer Therapy. *Mater. Today* **2011**, *14*, 316−323.
(7) O'Connell, M. J.; Bachilo, S. M.; Huffman, C. B.; Moore, V. C.; Strano, M. S.; Haroz, E. H.; Rialon, K. L.; Boul, P. J.; Noon, W. H.; Kittrell, C.; et al. Band Gap Fluorescence from Individual Single-Walled Carbon Nanotubes. *Science* **2002**, *297*, 593−596.
(8) Freitas, R. A., Jr. Pharmacytes: An Ideal Vehicle for Targeted Drug Delivery. *J. Nanosci. Nanotechnol.* **2006**, *6*, 2769−2775.
(9) Smith, B. W.; Monthioux, M.; Luzzi, D. E. Encapsulated C-60 in Carbon Nanotubes. *Nature* **1998**, *396*, 323−324.
(10) Vizuete, M.; Barrejon, M.; Gomez-Escalonilla, M. J.; Langa, F. Endohedral and Exohedral Hybrids Involving Fullerenes and Carbon Nanotubes. *Nanoscale* **2012**, *4*, 4370−4381.
(11) Okada, S.; Saito, S.; Oshiyama, A. Energetics and Electronic Structures of Encapsulated $C_{60}$ in a Carbon Nanotube. *Phys. Rev. Lett.* **2001**, *86*, 3835−3838.
(12) Xue, Q.; Jing, N.; Chu, L.; Ling, C.; Zhang, H. Release of Encapsulated Molecules from Carbon Nanotubes Using a Displacing Method: A MD Simulation Study. *RSC Adv.* **2012**, *2*, 6913−6920.
(13) Gao, H.; Kong, Y.; Cui, D.; Ozakan, C. S. Spontaneous Insertion of DNA Oligonucleotides into Carbon Nanotubes. *Nano Lett.* **2003**, *3*, 471−473.
(14) de Vos, R. M.; Verweij, H. High-Selectivity, High-Flux Silica Membranes for Gas Separation. *Science* **1998**, *279*, 1710−1711.
(15) Thomson, K. T.; Wentzcovitch, R. M. A Density Functional Study of the Electronic Structure of Sodalite. *J. Chem. Phys.* **1998**, *108*, 8584−8588.
(16) Yildirim, Y.; Hughes, R. The Efficient Combustion of O-Xylene in a Knudsen Controlled Catalytic Membrane Reactor. *Process Saf. Environ. Prot.* **2002**, *80*, 159−164.
(17) Molz, E.; Wong, A. P. Y.; Chan, M. H. W.; Beamish, J. R. Freezing and Melting of Fluids in Porous Glasses. *Phys. Rev. B* **1993**, *48*, 5741−5750.
(18) Chaban, V. V.; Prezhdo, O. V. Water Boiling Inside Carbon Nanotubes: Toward Efficient Drug Release. *ACS Nano* **2011**, *5*, 5647−5655.
(19) Chaban, V. V.; Prezhdo, V. V.; Prezhdo, O. V. Confinement by Carbon Nanotubes Drastically Alters the Boiling and Critical Behavior of Water Droplets. *ACS Nano* **2012**, *6*, 2766−2773.
(20) Panczyk, T.; Jagusiak, A.; Pastorin, G.; Ang, W. H.; Michalek, J. N. Molecular Dynamics Study of Cisplatin Release from Carbon Nanotubes Capped by Magnetic Nanoparticles. *J. Phys. Chem. C* **2013**, *117*, 17327−17336.
(21) Partha, R.; Conyers, J. L. Biomedical Applications of Functionalized Fullerene-Based Nanomaterials. *Int. J. Nanomed.* **2009**, *4*, 261−275.
(22) Bakry, R.; Vallant, R. M.; Haq, M. N.; Rainer, M.; Szabo, Z.; Huck, C. W.; Bonn, G. K. Medicinal Applications of Fullerenes. *Int. J. Nanomed.* **2007**, *2*, 639−649.
(23) Baweja, L.; Gurbani, D.; Shanker, R.; Pandey, A. K.; Subramanian, V.; Dhawan, A. C60-Fullerene Binds with the ATP Binding Domain of Human DNA Topoiosmerase II $\alpha$. *J. Biomed. Nanotechnol.* **2011**, *7*, 177−178.
(24) Hess, B.; Kutzner, C.; van der Spoel, D.; Lindahl, E. GROMACS 4: Algorithms for Highly Efficient, Load-Balanced, and Scalable Molecular Simulation. *J. Chem. Theory. Comput.* **2008**, *4*, 435−447.
(25) Chaban, V. V.; Savchenko, T. I.; Kovalenko, S. M.; Prezhdo, O. V. Heat-Driven Release of a Drug Molecule from Carbon Nanotubes: A Molecular Dynamics Study. *J. Phys. Chem. B* **2010**, *114*, 13481−13486.
(26) Hirahara, K.; Bandow, S.; Suenaga, K.; Kato, H.; Okazaki, T.; Shinohara, H.; Iijima, S. Electron Diffraction Study of One-Dimensional Crystals of Fullerenes. *Phys. Rev. B* **2001**, *64*, 115420−115425.
(27) Troche, K. S.; Sato, F.; Coluci, V. R.; Legoas, S. B.; Braga, S. F.; Rurali, R.; Chinellato, D. D.; Galvão, D. S. Prediction of Ordered Phases of Encapsulated $C_{60}$, $C_{70}$, and $C_{78}$ Inside Carbon Nanotubes. *Nano Lett.* **2005**, *5*, 349−355.
(28) Pickett, G. T.; Gross, M.; Okuyama, H. Spontaneous Chirality in Simple Systems. *Phys. Rev. Lett.* **2000**, *85*, 3652−3655.